2004

Experimental Study on R-410A Condensation Heat Transfer and Pressure Drop Characteristics in Oblong Shell and Plate Heat Exchanger

Jae Hong Park
PuKyong National University

Yong Chan Ha Kwon
PuKyong National University

Young Soo Kim
PuKyong National University

EXPERIMENTAL STUDY ON R-410A CONDENSATION HEAT TRANSFER AND PRESSURE DROP CHARACTERISTICS IN OBLONG SHELL AND PLATE HEAT EXCHANGER

Jae-Hong Park[1], Yong-Ha Kwon[2], Young-Soo Kim[3]

[1]Pukyong Natl. Univ., Refrigeration and Air-Conditioning Engineering,
#100 Yongdang-Dong, Nam-Gu, Busan, Korea, 608-739
+80-51-620-1503, +82-51-623-8495, parksonforever@hanmail.net

[2]Pukyong Natl. Univ., Refrigeration and Air-Conditioning Engineering,
#100 Yongdang-Dong, Nam-Gu, Busan, Korea, 608-739
+80-51-620-1503, +82-51-623-8495, bekpye@hotmail.com

[3]Pukyong Natl. Univ., School of Mechanical Engineering,
#100 Yongdang-Dong, Nam-Gu, Busan, Korea, 608-739
+80-51-620-1503, +82-51-623-8495, yskim@pknu.ac.kr

ABSTRACT

In this study, condensation heat transfer experiments were conducted with oblong shell and plate heat exchanger (OSPHE) using R-410A. An experimental refrigerant loop has been established to measure the condensation heat transfer coefficient h_r and frictional pressure drop ΔP_f of R-410A in a vertical OSPHE. Four vertical counter flow channels were formed in the OSPHE by five plates of geometry with a corrugated trapezoid shape of a chevron angle of 45 degree. OSPHE is different from the conventional plate heat exchanger. The plates that have an oblique pattern are elliptical in shape and stacked together in contrary arrangements, which are enclosed in a cylindrical shell. Although OSPHE is different from the conventional rectangular plate heat exchanger, the underlying flow channels through heat exchanger are the same as the conventional plate heat exchanger. The effects of the refrigerant mass flux, average heat flux, refrigerant saturation temperature and vapor quality of R-410A on the measured data were explored in detail. The results indicate that the condensation heat transfer coefficients and pressure drops increase with the vapor quality. A rise in the refrigerant mass flux causes an increase in the h_r and ΔP_f. Also, a rise in the average heat flux causes an increase in the h_r. But the effect of the average heat flux does not show significantly effect on the ΔP_f. Finally, at a higher saturation temperature the h_r is found to be lower. On the other hand, the effect of the saturation temperature on the ΔP_f is small. Based on the present data, the empirical correlations are also provided for the measured heat transfer coefficients and pressure drops in terms of the Nusselt number and friction factor.

1. INTRODUCTION

Many air-conditioning and refrigeration systems have long used R-22 as the working fluid. Recently, because of the phase-out of CFCs and HCFCs outlined by the Montreal Protocol, R-22 will be phased out early this century. As a result, the search for a replacement for R-22 has been intensified in recent years. R-410A, a mixture of 50 wt% R-32 and 50 wt% R-125 that exhibits azeotropic behavior has been considered one of the primary replacements for R-22 in air-conditioning and refrigeration system applications. Moreover, in view of space saving and tightening energy-efficiency standards imposed by the federal government, the design of more compact heat exchangers is relatively important. Also, to meet the demand for saving energy and resources today, manufacturers are trying to enhance efficiency and reduce the size and weight of heat exchangers. Over the past decade, there has been tremendous advancement in the manufacturing technology of high efficiency heat exchangers. This has allowed the use of smaller and high performance heat exchangers. Consequently, the use of smaller and high performance heat exchanger will become popular in the design of HVAC heat exchangers. Normally, these heat exchangers are used in the two phase system for evaporation and condensation. In the design and analysis of the two phase system within this heat exchanger, it is necessary to understand the flow field and frictional characteristics of the two phase system.

When compared with the well-established shell and tube heat exchangers, the plate heat exchanger shows a lot of advantages like high *NTU* values, compactness, low cost, multi duties and reduced fouling etc. Plate heat exchangers have been widely used in food processing, chemical reaction processes, and other industrial applications for many years. Particularly, in the last 30 years plate heat exchangers have been introduced to the refrigeration and air conditioning systems as evaporators or condensers for their high efficiency and compactness.

The Oblong Shell and Plate heat exchanger (OSPHE) is different from the conventional plate heat exchanger. The plates that have an oblique pattern are ellipse in shape, and stacked together in contrary arrangements, which are enclosed in a cylindrical shell. The operating temperature rises up to 350℃, and the pressure up to 10 MPa can be achieved. Although OSPHE is different from the conventional rectangular plate heat exchanger, the underlying flow channels through the exchanger are the same as the conventional plate heat exchanger. So OSPHE is being introduced to refrigeration and air conditioning systems as evaporators or condensers for their high efficiency and compactness. However, there are little data available for the design of OSPHE used as evaporators and condensers.

In this study, the characteristics of the condensation heat transfer for R-410A flowing in the OSPHE were experimentally explored to set up data base for the design of the OSPHE.

2. EXPERIMENTAL APPARATUS AND PROCEDURES

2.1 Experimental apparatus

The experimental system and heat transfer plate used to study the condensation of R-410A are schematically shown in Fig. 1 and 2, respectively. The experimental system consisted of with a test section, a refrigerant loop, a water loop and a data acquisition unit. R-410A is circulated in a refrigerant loop. In order to obtain different test conditions of R-410A including the vapor quality, saturation temperature (pressure) and imposed heat flux in the test, we needed to control the temperature and flow rate of the working fluid in the water loop.

The Oblong Shell and Plate heat exchanger used in this study was formed by five commercialized SUS-304 plates. The plate surfaces were pressed to become grooved with a corrugated trapezoid shape and 45 deg of chevron angle. The corrugated grooves on the right and left outer plates have an oblique shape but those in the middle plate have a contrary oblique shape on both sides. Due to the contrary oblique shapes the flow streams near the plates cross each other in each channel. This cross flow creates a significant unsteady and random flow. In fact, the flow is highly turbulent even at low Reynolds number.

The refrigerant loop contains a refrigerant pump, a pre-heater, a test section (OSPHE), a sub-cooler, a strainer, a refrigerant mass flow meter, a dryer/filter, and five sight glasses. The refrigerant pump is a magnetic pump (TUTHILL California) driven by a DC motor which is, in turn, controlled by a variable DC output motor controller. The variation of the liquid R-410A flow rate was controlled by the rotational speed of DC motor through the change of the DC current. The refrigerant flow rate was measured by a mass flow meter (Oval) installed between the pump and receiver with an accuracy of ± 0.2%. The pre-heater is used to evaporate the refrigerant to a specified vapor quality at the test section inlet by transferring heat to R-410A. The amount of heat transfer from the pre-heater to refrigerant is measured by a power meter (YOKOGAWA) connected to the pre-heater source. The dryer/filter intends to filter the solid particles possibly present in the loop. Meanwhile, a sub-cooler was used to condense the refrigerant vapor flowing out the test section by a cold water to avoid cavitations at the pump inlet. The pressure of the refrigerant loop can be controlled by varying the temperature and flow rate of cold water in the sub-cooler. After condensed, the sub-cooled liquid refrigerant flows back to the receiver.

The water loop in the system, which is designed for circulating cold water through the test section, has a 200 liter constant temperature water bath equipped with a 5 kW heater and an air cooled refrigerant unit of 2 RT cooling capacity for accurate control of water temperature. The cold water is driven by a 0.37 kW water pump with an inverter to the OSPHE with a specified water flow rate. The accuracy of water flow rate measurement by the flow meter is ± 0.2%.

The water loop for condensing R-410A vapor has a 200 liter constant temperature water bath equipped with a 5 kW heater and an air cooled refrigeration unit of 3 RT cooling capacity for accurate control of water temperature. A 0.37 kW water pump with an inverter is used to drive the cold water at a specified water flow rate to the sub-cooler.

The data acquisition unit includes the 20 channels Fluke NetDAQ 2640A recorder combined with a personal computer. The recorder was used to record the temperature and voltage data. The NetDAQ 2640A recorder allows the measured data to transmit to personal computer and then to be analyzed by the computer immediately.

2.2 Experimental procedures

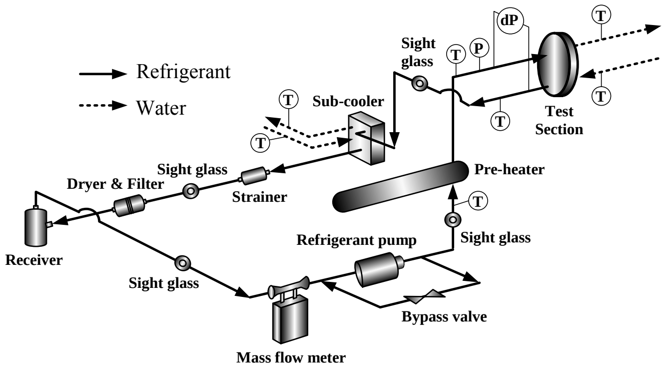

Figure 1 : Schematic diagram of Oblong Shell and Plate heat exchanger

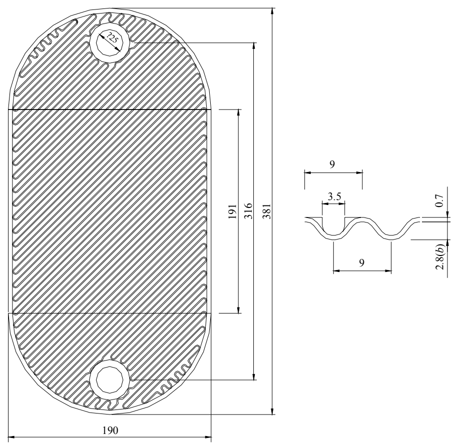

Figure 2 : Schematic diagram of heat transfer plate

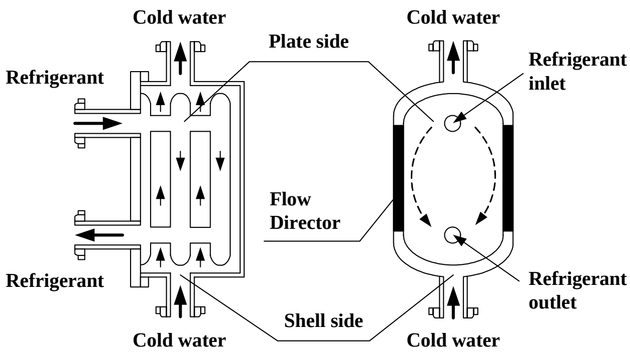

Figure 3 : Details of condensation flow direction

In each test pressure of the refrigerant loop can be controlled by varying the temperature and flow rate of the water loop in the sub-cooler and current in the pre-heater. The vapor quality of R-410A at the test section inlet can be kept at the desired value by adjusting the voltage of the voltage transformer for the pre-heater. The heat transfer rate between the counter flow channels in the test section can be varied by changing the temperature and flow rate in the water loop for the test section. Any change of the system variables will lead to fluctuations in the temperature and pressure of the flow. It takes about 60-120 min to reach a statistically steady state at which variations of the time-average inlet and outlet temperatures are less than 0.1℃ and the variations of the pressure and heat flux are within 1% and 5%, respectively. Then the data acquisition unit is initiated to scan all the data channels for 30 times in 5 min. The mean values of the data for each channel are obtained to calculate the heat transfer coefficient.

Before examining the condensation heat transfer characteristics, the preliminary experiments for single phase water convection in the plate and shell heat exchangers were performed. The modified Wilson's method (Farrell et al., 1991) was adopted to calculate the relation between single phase heat transfer coefficient and flow rate from these data. This single phase heat transfer coefficients can then be used to analyze the data acquired from the two-phase heat transfer experiments.

3. DATA REDUCTION

From the definition of the hydraulic diameter, Shah and Wanniarachchi (1992) suggested to use two times of the channel spacing as the hydraulic diameter for plate heat exchangers when the channel width is much larger than the channel spacing. So we follow this suggestion.

$$d_h \approx 2b \tag{1}$$

3.1 Two phase condensation heat transfer

The total heat transfer rate between the counter flows in the test section is calculated from the cold water side as

$$Q_w = m_{w,c} c_{p,w} (T_{w,c,o} - T_{w,c,i}) \tag{2}$$

Then, the refrigerant vapor quality entering the test section is evaluated from the energy balance for the pre-heater. The heat transfer to the refrigerant in the pre-heater is the sum of the sensible heat transfer (for the temperature rise of the refrigerant to the saturated value) and latent heat transfer (for the evaporation of the refrigerant).

$$Q_p = Q_{sens} + Q_{lat} \tag{3}$$

$$Q_{sens} = m_r c_{p,r} (T_{r,sat} - T_{r,p,i}) \tag{4}$$

$$Q_{lat} = m_r i_{fg} x_{p,o} \tag{5}$$

The above equations can be combined to evaluate the refrigerant quality at the exit of pre-heater that is considered to be the same as the vapor quality of refrigerant entering the test section. Specifically,

$$x_i = x_{p,o} = \frac{1}{i_{fg}} \left(\frac{Q_p}{m_r} - c_{p,r} (T_{r,sat} - T_{r,p,i}) \right) \tag{6}$$

The change in the refrigerant vapor quality in the test section is then deduced from the heat transfer to the refrigerant in the test section,

$$\Delta x = \frac{Q_w}{m_r \cdot i_{fg}} \tag{7}$$

The average quality in the test section is given as

$$x_{ave} = x_m = x_i - \frac{\Delta x}{2} \tag{8}$$

The overall heat transfer coefficient U for the counter flow between the two channels can be expressed as

$$U = \frac{Q_w}{A \cdot LMTD} \tag{9}$$

where $LMTD$ is the logarithmic mean temperature difference between the two channels defined as

$$LMTD = \frac{(\Delta T_1 - \Delta T_2)}{\ln(\Delta T_1 / \Delta T_2)} \tag{10}$$

where

$$\Delta T_1 = T_{r,sat,o} - T_{w,c,i} \tag{11}$$

$$\Delta T_2 = T_{r,sat,i} - T_{w,c,o} \tag{12}$$

with $T_{r,sat,i}$ and $T_{r,sat,o}$ are the saturation temperatures of R-410A corresponding respectively to the inlet and outlet pressures in the P&SHE. Finally, the condensation heat transfer coefficient of R-410A is evaluated from

$$\left(\frac{1}{h_r} \right) = \left(\frac{1}{U} \right) - \left(\frac{1}{h_{w,c}} \right) - R_{wall} A \tag{13}$$

where the modified Wilson plot method was applied to calculate $h_{w,c}$.

3.2 Two phase condensation pressure drop

To evaluate the frictional pressure drop associated with the R-410A condensation in the refrigerant channel, the frictional pressure drop ΔP_f was calculated by subtracting the pressure losses at the test section inlet and exit manifolds and ports $(\Delta P)_{man}$, then adding the deceleration pressure rise during the R-410A condensation ΔP_{de} and the elevation pressure rise ΔP_{ele} from the measured total pressure drop ΔP_{exp} for the refrigerant channel. Note that for the vertical downward refrigerant flow studied here the elevation pressure rise should be added in evaluating ΔP_f. Thus

$$\Delta P_f = \Delta P_{\exp} - (\Delta P)_{man} + \Delta P_{de} + \Delta P_{ele} \tag{14}$$

The deceleration and elevation pressure rises were estimated by the homogeneous model for two phase gas-liquid flow.

$$\Delta P_{de} = G^2 \upsilon_{fg} \Delta x \tag{15}$$

$$\Delta P_{ele} = \frac{gL}{\upsilon_m} \tag{16}$$

where υ_m is the mean specific volume of the vapor-liquid mixture in the refrigerant channel when they are homogeneously mixed and is given as

$$\upsilon_m = [x_m \upsilon_g + (1 - x_m)\upsilon_f] = (\upsilon_f + x_m \upsilon_{fg}) \tag{17}$$

The pressure drop in the inlet and outlet manifolds and ports was empirically suggested by Shah and Focke (1988). It is approximately 1.5 times the head due to the flow expansion at the channel inlet

$$(\Delta P)_{man} = 1.5\left(\frac{u_m^2}{2\upsilon_m}\right)_i \tag{18}$$

where u_m is the mean flow velocity. With the homogeneous model the mean velocity is

$$u_m = G\upsilon_m \tag{19}$$

Based on the above estimation the deceleration pressure rise, the pressure losses at the test section inlet and exit manifolds and ports, and the elevation pressure rise were found to be rather small. The frictional pressure drop ranges from 95% to 99% of the total pressure drop measured. According to the definition

$$f_{tp} \equiv -\left(\frac{\Delta P_f d_h}{2G^2 \upsilon_m L}\right)_i \tag{20}$$

4. RESULTS AND DISCUSSION

4.1 Single phase heat transfer

From the initial single phase water to water heat transfer test for the OSPHE, the convection heat transfer coefficient in the shell side was correlated as

$$Nu_s = 0.05\,\mathrm{Re}^{0.95}\,\mathrm{Pr}^{1/3} \tag{21}$$

The energy balance between the hot and cold side of water was within 3% for all runs.

4.2 Two phase heat transfer

In the present investigation of the R-410A condensation in the P&SHE, the R-410A mass flux G was varied from 40 to 80 kg/m^{2}s, the average heat flux q_w'' from 4.0 to 8.0 kW/m^2 and the saturation temperature $T_{r,sat}$ from 30 to 40℃. The measured heat transfer coefficients are to be presented in terms of their variations with the average vapor quality in the test section.

Figure 4 shows the effect of the refrigerant mass flux on the measured condensation heat transfer coefficients, where the measured data for G = 40, 60 and 80 kg/m^{2}s at $T_{r,sat}$ = 30℃ and q_w'' = 6.0 kW/m^2 is plotted as a function of x_m. The results show that the condensation heat transfer coefficient rises linearly with the mass flux in the total vapor quality region. This obviously results from the simple fact that at a higher x_m the liquid film on the surface is thinner and the condensation rate is thus higher.

The effects of average heat flux on the condensation heat transfer are shown Fig. 5 by plotting the measured data for q_w'' = 4, 6 and 8 kW/m^2 at G = 60 kg/m^{2}s and $T_{r,sat}$ = 30 °C as a function of x_m. It is well known that the condensation rate is almost proportional to the heat flux. The results indicate that at a given vapor quality the heat transfer coefficient is higher for a higher heat flux. However, compared with the mass flux effects shown in Fig. 4, the heat flux has a small effect on the condensation heat transfer coefficient in the whole vapor quality region.

The effect of the refrigerant saturation temperature on the condensation heat transfer coefficient is illustrated in Fig. 6 by plotting the data for $T_{r,sat}$ = 30, 35 and 40°C at G = 60 kg/m^{2}s and q_w'' = 6 kW/m^2 as a function of x_m. The results suggest that at a given saturation temperature the condensation heat transfer coefficient increases with the mean vapor quality. At a fixed x_m, the condensation heat transfer coefficient is lower for a higher $T_{r,sat}$ in the whole quality region. Specifically, the mean heat transfer coefficient at 30℃ is about 15% bigger than that at 40℃. This is conjectured to be mainly resulting from reduction in the conductivity of liquid film for the R-410A saturation temperature raised from 30 to 40℃. The associated thermal resistance of the liquid film is larger, causing a poorer heat transfer rate.

It is necessary to compare the present data for the R-410A condensation heat transfer coefficient in the OSPHE to those in plate heat exchanger reported in the literature. Due to the limited availability of the data for plate heat exchangers with the same range of the parameters covered in the present study, the comparison is only possible for a few cases. This is illustrated in Fig. 7, in which our data are compared with correlation of Yan et al. (1999) and our R-134a data in the same test section. Note that the data from Yan et al. are R-134a condensation heat transfer coefficient measured in a plate heat exchanger with the vapor quality from 0.08 to 0.86. Yan et al. proposed condensation heat transfer correlation equation such as

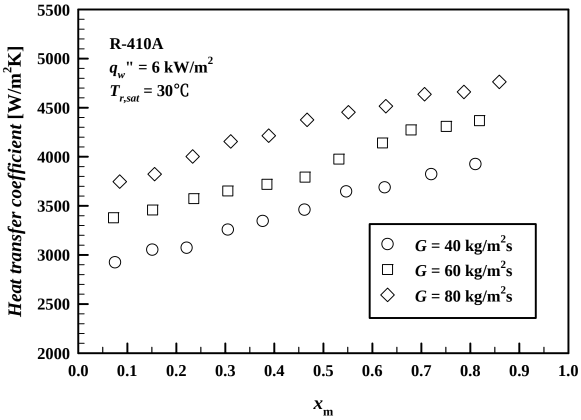

Figure 4 : Variations of condensation heat transfer coefficient with mean vapor quality for various mass fluxes at q_w'' = 6.0 kW/m^2 and $T_{r,sat}$ = 30℃

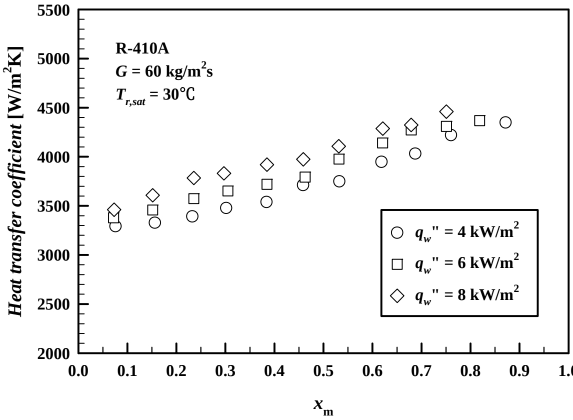

Figure 5 : Variations of condensation heat transfer coefficient with mean vapor quality for various heat fluxes at G = 60 kg/m^{2}s and $T_{r,sat}$ = 30℃

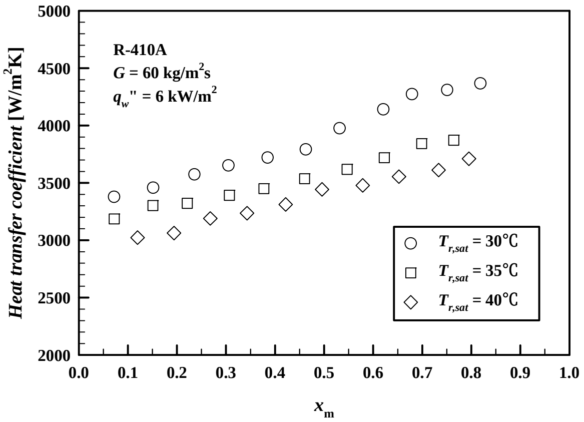

Figure 6 : Variations of condensation heat transfer coefficient with mean vapor quality for various saturation temperatures at G = 60 kg/m^{2}s and q_w'' = 6.0 kW/m^2

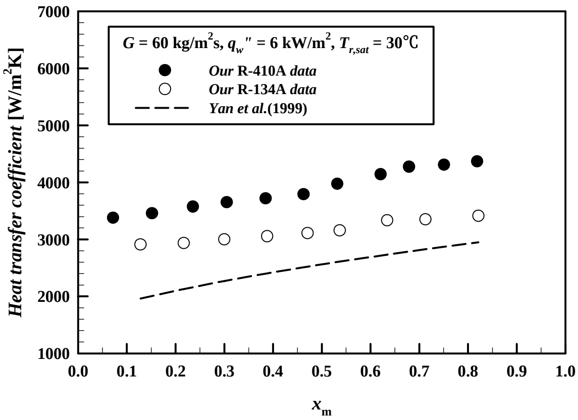

Figure 7 : Comparison of the present heat transfer data with those for plate heat exchanger from Yan et al. and our R-134A data

$$Nu = h_r \frac{d_h}{k_l} = 4.118\,\mathrm{Re}_{eq}^{0.4} \tag{22}$$

where Re_{eq} is the equivalent Reynolds number. Re_{eq} is defined as

$$\mathrm{Re}_{eq} = \frac{G_{eq} d_h}{\mu_l} \tag{23}$$

and G_{eq} is the equivalent mass flux first proposed by Akers et al. (1958) defined as

$$G_{eq} = G\left[1 - x_m + x_m\left(\frac{\rho_l}{\rho_\upsilon}\right)^{1/2}\right] \tag{24}$$

The comparison shows that the R-410A condensation heat transfer coefficient for OSPHE is about 23% higher in average than that for our R-134A experiment. Also, the comparison indicates that our R-134A condensation heat transfer coefficient for OSPHE is about 26% higher than that for the plate heat exchanger.

4.3 Two phase pressure drop

Figure 8 shows the effect of the refrigerant mass flux on R-410A frictional pressure drop. The results indicate that at a given mass flux the pressure drop is larger for a higher vapor quality. In addition, the pressure drop with the vapor quality is more pronounced for a higher mass flux. This obviously results from the simple fact that at a higher x_m the velocity of vapor was larger and the pressure drop was thus higher.

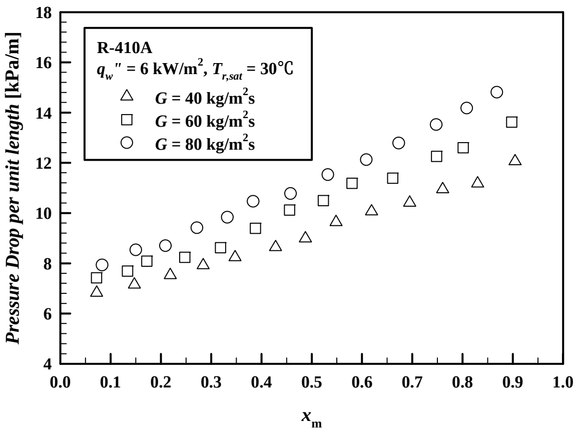

Figure 8 : Frictional pressure drop variation with the mean vapor quality for various mass fluxes at $q_w'' = 6.0$ kW/m^2 and $T_{r,sat} = 30$°C

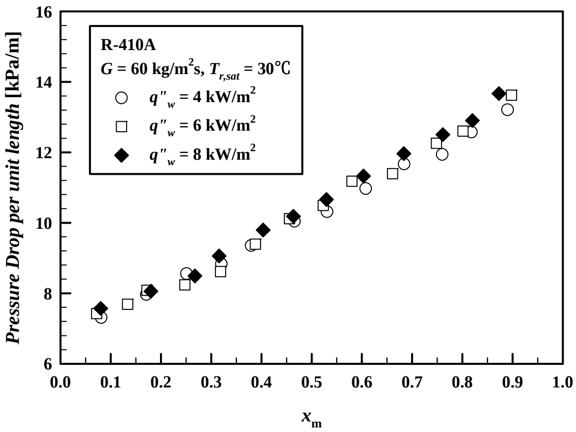

Figure 9 : Frictional pressure drop variation with the mean vapor quality for various heat fluxes at $G = 60$ kg/m^{2}s and $T_{r,sat} = 30$°C

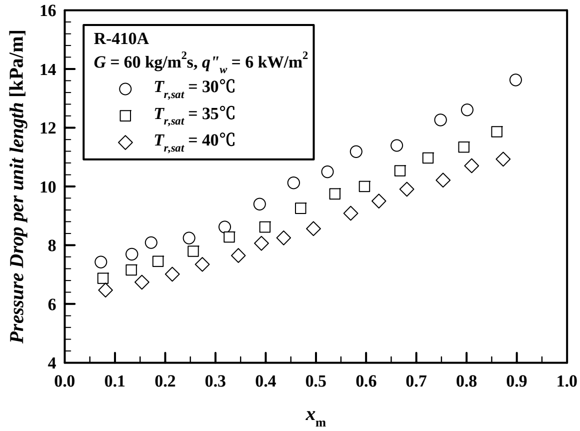

Figure 10 : Frictional pressure drop variations with the mean vapor quality for various saturation temperatures at $G = 60$ kg/m^{2}s and $q_w'' = 6.0$ kW/m^2

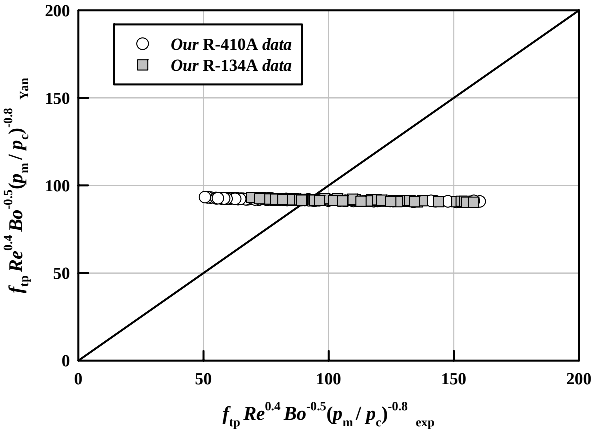

Figure 11 : Comparison of the present pressure drop data with those for plate heat exchanger from Yan et al.

Figure 9 shows the effects of the heat flux on the frictional pressure drop. The data indicate that at a given heat flux the frictional pressure drop increases linearly with the mean vapor quality of the refrigerant in the P&SHE. But an increase in the heat flux dose not show significantly effect on the frictional pressure drop in the OSPHE.

The results in Fig. 10 for different saturation temperatures of R-410A indicated that at a given $T_{r,sat}$ the pressure drop is larger for a higher vapor quality. Note that in the total vapor quality range the pressure drop is smaller at a higher $T_{r,sat}$. This is conjectured to be mainly resulting from a reduction in the velocity of vapor for the R-410A saturation temperature raised from 30 to 40°C.

Figure 11 compares the condensation pressure drop for both the OSPHE and plate heat exchanger from Yan et al. (1999).

4.4 Correlation equations

To facilitate the use of the Oblong Shell and Plate heat exchanger as condensers, correlating equations for the dimensionless condensation heat transfer coefficient and friction factor based on the present data are provided. This is the modified Yan et al's correlation.

$$Nu = h_r \frac{d_h}{k_l} = 14.73\, \mathrm{Re}_{eq}^{0.281}\, \mathrm{Pr}_l^{1/3} \;,\; 2300 < \mathrm{Re}_{eq} < 13200 \tag{25}$$

$$f_{tp}\, \mathrm{Re}^{0.4}\, Bo^{-0.5} \left(\frac{P}{P_c}\right)^{-0.8} = 2.675\times10^{6}\, \mathrm{Re}_{eq}^{-1.176},\; 2300 < \mathrm{Re}_{eq} < 13200 \tag{26}$$

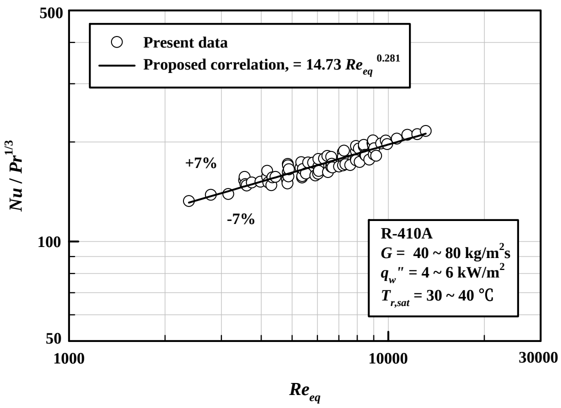

Figure 12 : Comparison of the proposed correlation for Nusselt number with the present data

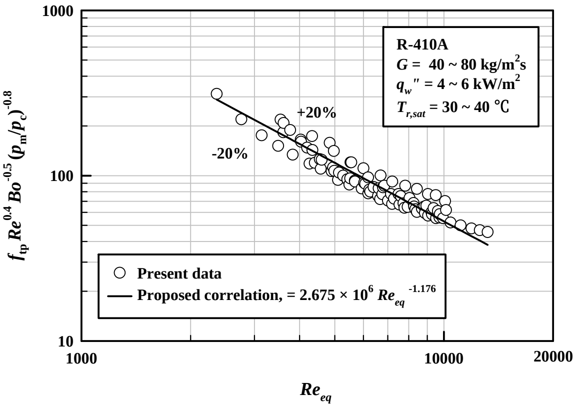

Figure 13 : Comparison of the proposed correlation for friction factor with the present data

where P_c is the critical pressure of R-410A.

Figure 12 shows the comparison of the proposed condensation heat transfer correlation to the present data, indicating that most of the experimental values are within ±7%. Figure 13 shows the comparison of the proposed correlation for the friction factor to the present data. It is found that the average deviation is about ±20% between f_{tp} correlation and the data.

5. CONCLUSIONS

An experiment has been carried out in the present study to measure the heat transfer coefficient and pressure drop for the condensation of R-410A flowing in the Oblong Shell and Plate heat exchanger. The effects of the mass flux of R-410A, average imposed heat flux, saturated temperature and vapor quality of R-410A on the measured data were experimentally examined in detail.

The present results for the OSPHE show that the condensation heat transfer coefficient and pressure drop normally increase with the refrigerant mass flux. A rise of heat flux dose not show significant effect on the condensation heat transfer coefficient and the frictional pressure drop at the whole vapor quality in the P&SHE. It was noted that at a higher saturation temperature of the refrigerant condensation heat transfer coefficient and pressure drop are lower. The empirical correlations are also provided for the measured heat transfer coefficients and pressure drop in terms of the Nusselt number and friction factor.

NOMENCLATURE

A : heat transfer area of the plate (m^2)
G : mass flux (kg/m^2s)
L : length from center of inlet port to center of exit port (m)

B_o : Boiling number
i_{fg} : enthalpy of vaporization (J/kg)
m : mass flow rate (kg/s)
Q : heat transfer rate (W)

Subscripts

p : pre-heater
r : refrigerant
w : water

REFERENCES

Akers, W. W., Dean, H. A. and Crosser, O., 1958, Condensation Heat Transfer Within Horizontal Tubes, *Chem. Eng. Prog.* 54, p. 89-90.

Farrell, P., Wert, K. and Webb, R., 1991, Heat Transfer and Friction Characteristics of Turbulent Radiator Tubes, *SAE Technical Paper series*, No. 910197.

Shah, R. K. and Focke, W. W., 1988, *Plate Heat Exchangers and Their Design Theory*, in: Shah, R. K., Subbarao, E. C. and Mashelkar, R. A.(Eds.), Heat Transfer Equipment Design, Hemisphere, Washington, DC, p. 227-254.

Shah, R. K. and Wanniarachchi, A. S., 1992, *Plate Heat Exchanger Design Theory in Industry Heat Exchanger*, in : J. -M. Buchlin(Ed.), Lecture Series, No, 1991-04, Von Karman Institute for Fluid Dynamics, Belgium.

Yi Yie Yan, Hsiang Chao Lio, and Tsing Fa Lin, 1999, Condensation Heat Transfer and Pressure Drop of Refrigerant R-134a in a Plate Heat Exchanger, *Int. J. Heat and Mass Transfer* 42, p. 993-1006.